Conducting polymer actuators as engineering materials

John D.W. Madden*, Peter G.A. Madden and Ian W. Hunter
Massachusetts Institute of Technology, Cambridge MA 02139

ABSTRACT

Conducting polymer actuators were first proposed more than ten years ago. Reported performance has improved dramatically, particularly in the past few years, due to changes in synthesis methods, better characterization and an understanding of the underlying mechanisms. These actuators are able to displace large loads (up to 100× greater than mammalian skeletal muscle), with moderate displacements (typically 2 %), and with power to mass ratios similar to that of muscle, while powered using potentials of no more than a few volts. Unlike electric motors and muscle, these actuators exhibit a catch state, enabling them to maintain force without consuming energy. Despite the impressive performance, commercial applications are at an early stage. One reason is the need to carefully consider the details of the actuator construction, including the thickness and surface area of the polymer, the electrolyte conductivity and geometry, the counter electrode spacing, the shape of the input voltage and the means of electrical contact to the polymer, in designing effective actuators. A set of design guidelines is presented that assist the device designer in determining the optimum actuator configuration. These are derived from extensive characterization and modeling of hexafluorophosphate-doped polypyrrole actuators. The set of design tools helps transform conducting polymer actuators into engineering materials that can be selected and designed for particular applications based on rational criteria. Most of the underlying physical principles used in determining these rules also underlie other conducting polymer actuators, polymer devices such as electrochromic displays, supercapacitors and batteries, carbon nanotube actuators, and electrochemically driven devices that involve volumetric charge storage.

Keywords: conducting polymer, actuator, polypyrrole, model, carbon nanotubes, impedance, diffusion.

1. INTRODUCTION

Conducting polymers are a class of materials that feature a conjugated backbone structure, Figure 1. These polymers exhibit chemically and electrochemically controllable electronic conductivities[1,2], which can match or exceed copper at $6 \cdot 10^7$ $S \cdot m^{-1}$, but usually do not exceed 10^5 $S \cdot m^{-1}$ in air stable materials. In the neutral state shown in Figure 1, the polymers are typically semiconductors. Oxidation or reduction creates delocalized charge carriers along the backbone leading to nearly metallic conduction in certain polypyrroles, polyanilines and polyacetylenes[1]. Figure 2 depicts such a change in oxidation state, induced electrochemically. During oxidation ions are inserted. These ions enter the polymer from a surrounding electrolyte and serve to balance charge.

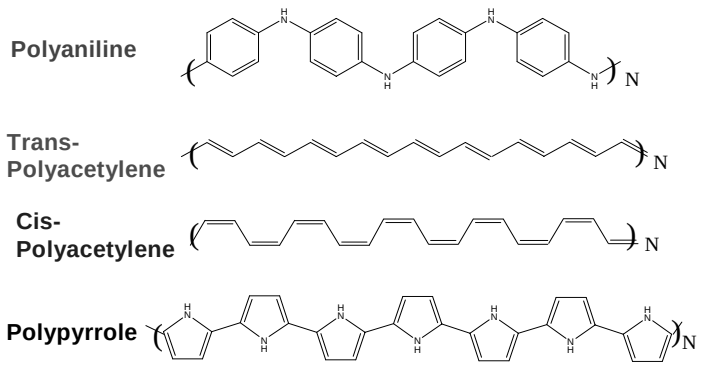

Figure 1: The chemical structures of some common conducting polymers.

In the process of changing oxidation state, conductivity, optical absorption, permeability, hydrophobicity and stored charge all change in a controllable manner, enabling chemical sensors, transistors, filters, capacitors, and batteries, among other devices, to be constructed[1]. Dimensional changes are also observed. These changes are the results of conformational changes, solvent insertion, ion insertion and electrostatic interactions[3]. In polypyrrole, one of the most widely studied conducting polymer actuators, expansion is observed as ions are inserted, and the magnitude of the expansion is proportional to the change in ion charge density [4-8]. This result suggests that intercalation of ions between polymer chains is at least partly responsible for swelling. New conducting polymers are being developed that

* jmadden@mit.edu; http://bioinstrumentation.mit.edu.

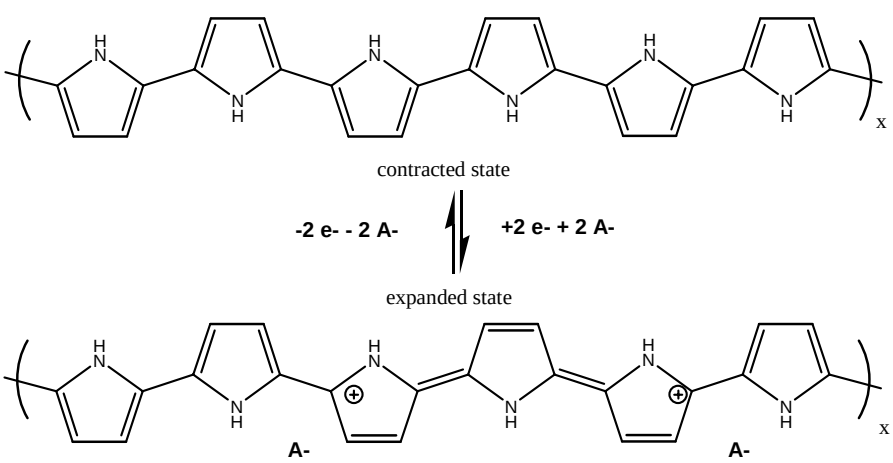

Figure 2: Electrochemical redox cycle for polypyrrole. A^- represent anions, e^- electrons.

undergo large conformation changes. These appear to create much larger strains, but are still at an early stage of characterization [9].

Conducting polymer actuators are of particular interest due to their low operating voltages, high forces, moderate strains, controllability and low cost. Cell voltages are often less than 2 V. Up to 10 V may be used over short periods to increase power[10]. The proportionality between displacement and charge makes control relatively easy. Forces exceed the 350 $kN \cdot m^{-2}$ of mammalian skeletal muscle[10] by up to two orders of magnitude[11], and, unlike mammalian muscle, virtually no energy expenditure is required to hold a load. The power to mass achieved so far is 39 $W \cdot kg^{-1}$ at strain rates of 3 $\%\cdot s^{-1}$ [8,10,12]. The power and strain rate is predicted to be substantially improved by reducing the size of films and fibers, as discussed below.

Conducting polymer actuators are a new technology, with particular characteristics that must be accounted for when incorporating them into a product. Typically conducting polymers are electrochemically driven, and therefore consideration must be given to encapsulation of the electrolyte, or use of a gel or dry ionic conductor [13]. Much of the input electrical energy is stored rather than converted to mechanical work. This stored energy needs to be recovered for high efficiency operation in moderate strain polymers such as polypyrrole and polyaniline. Methods of creating mechanical amplification of the strains, and of matching load mechanical impedance need to be considered. In this paper the focus is on choosing the appropriate volume, cross-section and film/fiber geometry to achieve the desired force, displacement, speed and power. Particular attention is paid to the factors limiting the rate of actuation, including mass transport and $R \cdot C$ charging. Most of these factors are common to other electrochemically activated devices, including carbon nanotube actuators.

The paper begins by reviewing the empirically and physically based models used to describe hexafluorophosphate-doped polypyrrole. These models are then used to help predict response as a function of polymer and electrolyte geometry, conductivity, polymer strain to charge ratio and capacitance. Similarities and differences between hexafluorophosphate-doped polypyrrole behavior and those of carbon nanotube actuators and other electrochemically driven devices are mentioned.

2. MODELS AND DESIGN IMPLICATIONS

A relatively simple relationship between stress, σ, strain, ε and charge per unit volume, ρ, is found to describe the behavior of polypyrrole and polyaniline actuators to first order [5,8,14]:

$$\varepsilon(s) = \alpha(s) \cdot \rho(s) + \frac{\sigma(s)}{S(s)}. \qquad 1$$

The equation has been written in the Laplace domain, with s representing the Laplace variable, and $S(s)$, the frequency dependent stiffness [8,11]. The strain to charge ratio, α, is analogous to a thermal expansion coefficient, but for charge rather than temperature. The strain to charge ratio is experimentally found to range between $0.3\text{-}5\times10^{-10}$ $m^3 \cdot C^{-1}$ for polypyrrole and polyaniline actuators [5,8,14]. It is relatively time and load independent for a given polymer, although recently some relaxation has been observed [15]. A new generation of conducting polymers that are designed from the molecular scale to create actuation, promise to generate at least an order of magnitude larger strain to charge ratio [9]. At loads of several megaPascals and below creep is relatively small, and the response is well described by:

$$\varepsilon(t) = \alpha \cdot \rho(t) + \frac{\sigma(t)}{E}, \qquad 2$$

where t is time, and E represents the elastic modulus. The modulus of hexafluorophosphate-doped polypyrrole is 0.8 GPa when wet [8,11].

A complete electromechanical description includes input voltage as well as strain, stress and charge. In many conducting polymers the relationship between voltage and charge or current is complex, even at equilibrium, due to changes in the nature of the thermodynamics as a function of oxidation state, which can range from quasi-Nernstian behavior to states of high inter-particle interaction, as in a capacitor [16-21]. In oxidation states where conductivity is high, it is not unusual to find that charge is proportional to applied potential over a potential range that can exceed 1 V [8,11,17,20-23]. In hexafluorophosphate-doped polypyrrole this capacitance is found to be proportional to volume, and have a value of C_V=1.3·10^8 F·m^{-3} [8,11]. At equilibrium the strain may then be expressed as:

$$\varepsilon(t) = \alpha \cdot C_V \cdot V + \frac{\sigma(t)}{E}, \qquad 3$$

where V is the potential applied to the polymer. In many conducting polymers and for voltage excursions beyond ~2 V in hexafluorophosphate doped polypyrrole, the capacitive relationship between voltage and charge does not hold. However, the density of charge that must be transferred during actuation is similar, which has important consequences for the rate of actuation, as discussed below. Before considering rate limiting mechanisms, some considerations in choosing maximum actuator load are presented.

2.1. Load

Conducting polymer actuators are able to actively deform at stresses of at least 34 MPa [11,15]. However, application of load induces elastic deformation and creep in polymers [8,11,12,15,24]. In order to maintain position control, the actuator must be able to compensate for both of these effects. Over short periods, only the elastic response need be considered. The elastic strain induced by load is simply the ratio of the load induced stress, σ, and the elastic modulus, E. This strain must be less than or equal to the maximum active strain, ε_{max}, in order for an actuator to maintain position:

$$\varepsilon_{max} \geq \frac{\sigma}{E}. \qquad 4$$

The maximum strain is typically 2 %, and given an elastic modulus of 0.8 GPa, the peak load for which elastic deformation can be compensated is approximately 16 MPa. However, holding such high loads even for a few minutes, can lead to substantial creep, as shown in Figure 3. The designer must determine the extent of elastic deformation and creep that is acceptable, and the time scale and cycle life of the actuator. Measured creep and stress-relaxation curves, and visco-elastic models will then assist in determining the appropriate upper bounds in actuator stresses.

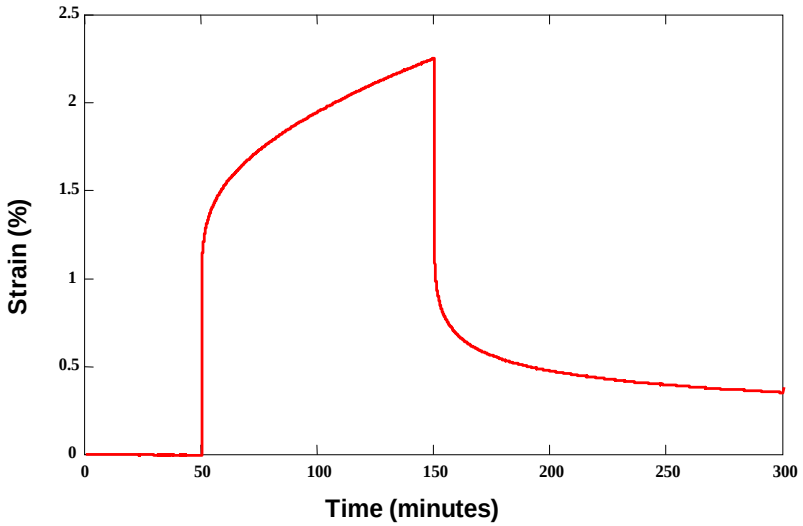

Figure 3: Creep in a polypyrrole film in response step in stress from 2 MPa to 20 MPa and back to 2 MPa. The test was performed in propylene carbonate with 0.05 M tetraethylammonium hexafluorophosphate.

Work and Actuator Volume

Most applications allow only limited volumes in which to fit an actuator, and usually smaller is better. In situations where a single actuator stroke is used to create motion, as in the action of the biceps muscle to displace the forearm, or of a hydraulic piston on a backhoe, the amount of work performed per stroke and per unit volume, u, is a key figure of merit. The actuator volume required, Vol_{min}, is then determined based on the work required per cycle, W:

$$Vol_{\min} \geq \frac{W}{u} \qquad 5$$

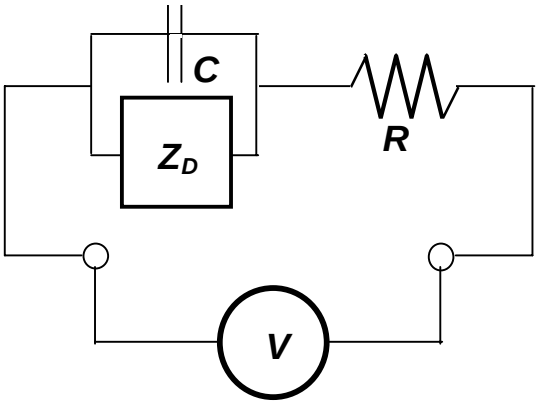

Figure 4: Equivalent circuit model of the actuator impedance. *V* represents an external voltage source, *C* the double layer capacitance, *R* the electrolyte/contact resistance, and Z_D, the diffusion impedance.

This volume is the minimum required, as energy delivery, sensors, linkages and often means of mechanisms of mechanical amplification generally also need to be incorporated.

In mammalian skeletal muscle, the work per unit volume is the product of the stress and strain. The maximum stress against which muscle can contract is 350 kPa, and the strain in vivo is 20 %, leading to a work density of 70 $J \cdot m^{-3}$. Strains in conducting polymer actuators are typically 1-2%. Thus although the stresses achievable in these actuators can exceed those of muscle by an order of magnitude or more, the overall work achieved per stroke approximately equal. At 5 MPa stress, and over a 2 % strain, the work density, typical of a hexafluorophosphate-doped polypyrrole actuator[8,11] is 100 $J \cdot m^{-3}$. Note that unlike muscle conducting polymers can perform work both under compression and tension, and therefore can generate a further doubling in work per volume in situations where this property is used.

2.2. Rate and Power

A given application will require a certain speed of response and delivery of power. In this section the factors limiting strain rate and power are presented as functions of actuator geometry, polymer and electrolyte conductivities, diffusion coefficients and capacitance. These equations enable the designer to determine physical and geometrical constraints necessary to achieve the desired performance.

Conducting polymers act as batteries or super-capacitors, storing tremendous quantities of charge per unit volume. In polypyrrole, for example, the capacitance is $C_V = 1.3 \times 10^8$ $F \cdot m^{-3}$, 5 orders of magnitude higher than a typical tantalum capacitor [11]. Strain is proportional to charge, and therefore the key to high strain rates and powers is to achieve high currents. Two factors limiting charging rate, namely internal resistance and mass transport, are discussed in detail, enabling the prediction of charging rates, and suggesting means of increasing speed through changes in actuator geometry and material properties.

Impedance, or its inverse, admittance, enable current and potential to be related. Figure 4 depicts an impedance model that contains features common to most electrochemically driven conducting polymer systems, and to many other electrochemical cells in which volumetric charging of an electrically conductive medium is occurring (e.g. carbon nanotube papers). In the model, *R*, represents the electrolyte resistance. *C* is the capacitance at the interface between the polymer and the electrolyte. Z_D is a diffusion element, modeling mass transport into the polymer. In the case of a planar geometry, as depicted in Figure 5, Z_D is expressed in the Laplace domain as:

$$Z_D(s) = \frac{\delta}{\sqrt{D \cdot C \cdot \sqrt{s}}} \cdot \coth\left(\frac{a}{2} \cdot \sqrt{\frac{s}{D}}\right). \qquad 6$$

where *D* is the diffusion coefficient, δ is the double layer thickness, *C* is the double layer capacitance and *a* is the polymer film thickness. Note that at low frequency the diffusion impedance reduces to:

$$Z_D = \frac{\delta}{a \cdot C \cdot s} = \frac{1}{C_V \cdot Vol}, \qquad 7$$

thereby behaving as a capacitance. The right hand expression restates the impedance in terms of the polymer capacitance per unit volume, C_V, and the polymer volume, *Vol*. Details of the derivation, assumptions and physical significance of the variables are provided in the Appendix of this paper.

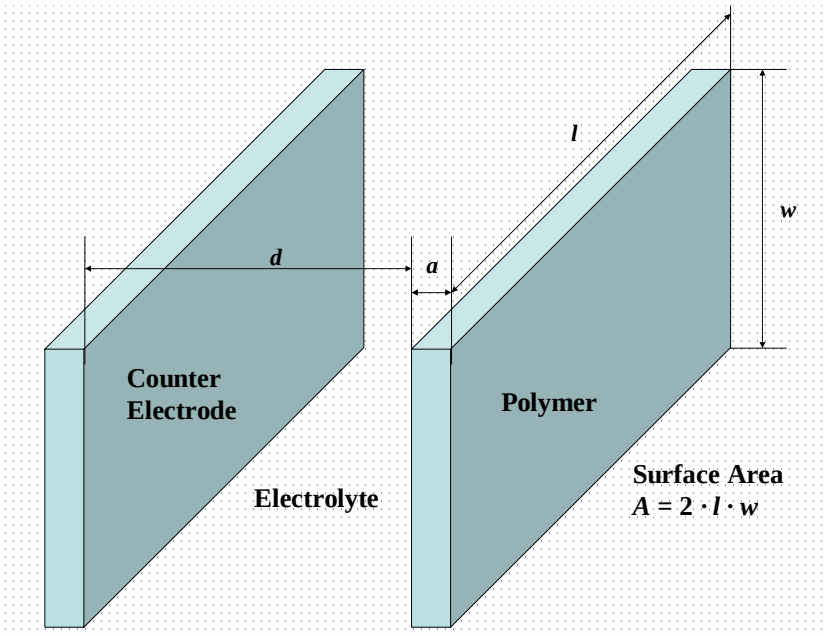

Figure 5: Dimensions of the polymer actuator. Electrical contact to the polymer is made at intervals of length *l*.

The model has been shown to provide a good description of hexafluorophosphate-doped polypyrrole impedance over a 2 V range, and at frequencies from 100 μHz up to 100 kHz[8,11]. It also reveals the rate limiting factors for charging, and hence actuation. One is the rate at which the double layer capacitance charges, which is limited by the internal resistance, *R*. A second is the rate of charging of the volumetric capacitor, which is determined by the slower of the rate of diffusion and the $R \cdot C_V \cdot Vol$ charging time. These time constants are discussed in detail below, as are the implications to the desired actuator geometry.

Before proceeding, it should be noted that the impedance model represented in Figure 4 is inappropriate in describing many conducting polymer electrochemical cells, and is not valid over all potentials. The polymer resistance is often higher than the electrolyte resistance, and can change significantly as a function of oxidation potential, producing an additional rate limiting mechanism. Reaction kinetics may limit the rate of charging, and the polymer may behave more like a battery than a capacitor, for example. However, all conducting polymers are capable of storing high charge densities, and the electronic and ionic charges must be transported throughout their volumes. Therefore maximizing rates of ionic and electronic transport in the polymer, and of ion transport in the adjacent electrolyte, are keys to rapid response. The time constants derived from the model in Figure 4 provide a starting point for understanding limits in all electrochemically driven conducting polymer systems.

Mechanisms of ion transport within the polymer can vary, and may include diffusion or convection through pores, molecular diffusion, or field induced migration along pores[5,11,17-23]. The mass transport model described by Equation 6 appears to represent only a diffusion response, and therefore to be restricted in its applicability. However, as explained in the Appendix, and depicted in Figure 6, the general form of Equation 6 provides a remarkably general description of ion and solvent transport within the polymer.

2.2.1. Double Layer Charging Time

Inspection of the model in Figure 4 suggests that no charge transfer can occur faster than the double layer charging time. If the double layer is not charged, there is no mechanism driving insertion of ions into the polymer, and therefore no displacement. The time constant for double layer charging, τ_{RC}, is:

$$\tau_{RC} = R \cdot C . \qquad 8$$

There are two primary sources of resistance – the electrolyte and the polymer. In order to maximize rate, the electrolyte

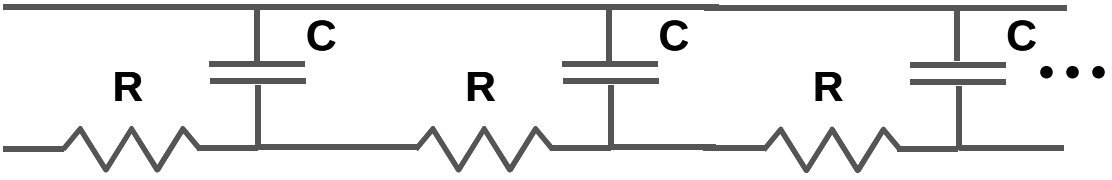

Figure 6: Diffusion represented by a transmission line model. The resistors may represent solution resistance, or fluid drag, and the capacitors double layer charging or electrolyte storage. This model also represents the charging of a polymer film whose resistance is significant compared to that of the adjacent electrolyte. In this case the resistance is that of the polymer, and the capacitance is the double layer capacitance or the volumetric capacitance.

ideally covers the polymer surface area, $A = 2 \cdot l \cdot w$, with as small an electrode separation, d, as possible. For example, when two planar electrodes are facing each other, the double layer charging time constant is:

$$\tau_{RC} = R \cdot C = \frac{d}{\sigma_e \cdot A} \cdot C = \frac{d}{\sigma_e} \cdot \frac{\partial C}{\partial A}. \quad 9$$

Typically the double layer capacitance[25] is in the range of 0.1 to 0.4 $F \cdot m^{-2}$, and, for a liquid electrolyte, it is usual to observe conductivities, σ_e, of approximately 1 to 10 $S \cdot m^{-1}$. In order to achieve a 1 ms response the separation, d, must be less than 100 mm for a 10 $S \cdot m^{-1}$ electrolyte.

The electrolyte resistance is commonly the primary source of cell resistance. However, for long films, poorly conductive polymers, or over a range of potentials where the conducting polymer is no longer in its quasi-metallic state, the film resistance can significantly limit rate. This factor is not accounted for in the model shown in Figure 4. In such a case, the combination of the film resistance and the double layer capacitance forms a transmission line, as depicted in Figure 6. The charging time constant can be re-expressed in terms of the polymer conductivity, σ_p, and the film length, l, width, w, and thickness, a:

$$\tau_{RCP} = R_p \cdot C = \frac{l^2}{4 \cdot \sigma_p \cdot a} \cdot \frac{\partial C}{\partial A}. \quad 10$$

This expression assumes that the polymer is electrically connected at both ends, and is multiplied by 4 when only one end is attached. In hexafluorophosphate-doped polypyrrole, conductivities typically exceed 10^4 $S \cdot m^{-1}$. In order to obtain a double layer charging time of 1 ms, the ratio of length squared divided by thickness must be less than 100. A 10 μm thick film contacted a both ends should be less than 60 mm long.

2.2.2. Volumetric Charging

It is relatively easy to obtain rapid charging of the double layer. However charging not only occurs at the surface, but also throughout the volume. Independent of the nature of the charge-voltage relationship (e.g. battery or capacitor), a certain charge density must be delivered through an internal resistance. For a battery-like response, the charging time is proportional to the internal resistance and the total charge. For capacitor-like behavior, as in hexafluorophosphate-doped polypyrrole, the time constant for volumetric charging, τ_{RCV}, is:

$$\tau_{RCV} = R \cdot C_V \cdot Vol = \frac{d \cdot a}{2 \cdot \sigma_e} \cdot C_V, \quad 11$$

in the case where electrolyte resistance is large compared to the polymer resistance. In order to charge a 10 μm thick film in 1 s and given and electrolyte conductivity of 10 $S \cdot m^{-1}$, the electrolyte dimension, d, must be less than 20 mm.

In the case where the polymer resistance is substantial compared to the electrolyte resistance, the volumetric charging time constant becomes:

$$\tau_{RCVP} = R_p \cdot C_V = \frac{l^2}{4 \cdot \sigma_p} \cdot C_V. \quad 12$$

The factor of 4 is appropriate only when both ends of the film are electrically connected. A 20 mm long film having a conductivity of 10^4 $S \cdot m^{-1}$ has a time constant of $\tau_{RCVP} = 1$ s.

The keys to improving $R \cdot C$ response times are to reduce the distance, l, between contacts, the distance between electrodes, d, and the polymer thickness, a. Maximizing electrolyte and polymer conductivities is also important. Finally, if the volumetric capacitance can be reduced without diminishing strain, the charge transfer is reduced. New polymers are being designed and tested whose strain to charge ratio is much larger, and capacitance is lower[9]. These polymers promise to charge faster while also developing greater strain, when compared to polypyrrole.

2.2.3. Resistance Compensation

Doubling the voltage input to a linear system leads to a doubling of the current. Why not increase the input voltage to achieve faster charging or discharging of the polymer? One reason not to is that extreme voltages at the electrolyte/polymer interface lead to degradation of the polymer and the electrolyte. Furthermore, the strain is proportional to the voltage at

equilibrium (e.g. Equation 3), so there is a risk of overshooting the target displacement. However, if the system is well modeled, then the double layer potential (across the capacitance, *C*, in Figure 4) can be estimated. It is this potential that in turn determines the charge state of the polymer, and therefore the extent of actuation. With the double layer potential estimated, the input potential can be shaped to maximize rate, while preventing excessive potential differences from developing across the double layer, and thereby avoiding degradation and overshoot[8,11].

One of the simplest cases where such an approach is desirable occurs when the electrolyte resistance is significantly greater than the polymer resistance. This case is very common in hexafluorophosphate-doped polypyrrole actuators, and is well modeled using the circuit shown in Figure 4. The polymer diffusion impedance, Z_D, and double layer capacitance, *C*, act as a low pass filter. The electrolyte resistance is then easily identified (e.g. using an impulse, step or high frequency sinusoidal input). The product of the current and the resistance, $I \cdot R$, then determines the drop across the electrolyte. Subtracting this voltage from the total applied potential, *V*, yields the double layer potential, V_{dl}. Assuming that the double layer potential is meant to reach but not exceed a voltage, V_{dl}^{max}, then the controller must simply maintain the input voltage such that:

$$V = V_{dl}^{max} - I \cdot R \,. \qquad 13$$

This method effectively eliminates the rate-limiting effects of the resistance, *R*, in Figure 4. The remaining rate limiting factors are then due to polymer resistance and mass transport. Note that in this method rate is increased at the expense of efficiency, as there is increased dissipation across the electrolyte.

2.2.4. Mass Transport

Ions must be transported within the polymer to balance charge during oxidation and reduction. Several mechanisms have been suggested to model this transport within the polymer, including molecular diffusion[8,11], conduction or diffusion through electrolyte filled pores[17-23], and convection through pores[5]. Although the mechanisms are different, the solutions share a common mathematical form, represented by Equation 4, and described by the finite transmission line of Figure 6. The charging time constant is:

$$\tau_D = \frac{a^2}{4 \cdot D}, \qquad 14$$

where *D* is the effective diffusion coefficient and *a* is the film thickness. The factor of 4 is removed if ions only have access from one side of the film. Diffusion coefficients in hexafluorophosphate-doped polypyrrole range[8,11] between 0.7 and 7×10^{-12} $m^2 \cdot s^{-1}$. In order to obtain a 1 s response time the polymer film thickness must be less than approximately 5 μm.

2.2.5. Summary

The primary rate limiting factors are volumetric charging times, (τ_{RCV} and τ_{RCVP}) and diffusion time (τ_D). These can be reduced by minimizing the distance between electrodes, *d*, the spacing between contacts, *l*, and the film thickness, *a*. Reduction of the thickness, *a*, and the length between contacts, *l*, is particularly effective at reducing diffusion time and volumetric charging time, as these time constants involve the squares of distances.

It is interesting to conjecture what the ultimate rate and power from conducting polymer actuators could be, assuming the optimum geometry can be constructed. A 10 nm thick polypyrrole actuator that is several micrometers long is predicted to exhibit a diffusion time constant of 3μs, be capable of strain rates of 3000 $\%\cdot s^{-1}$, and of power to mass ratios of 30 $kW \cdot kg^{-1}$, 30× greater than an internal combustion engine. Is this realistic? Results from other electrochemically activated conducting polymer devices suggest that such rate and power are possible. Conducting polymer transistors and electrochromic devices have been electrochemically cycled at tens of kilohertz[2,26]. These high frequencies are achieved by employing films that are several tens of nanometers thick.

2.3. Notes on Potential Application to Carbon Nanotube Actuators

Carbon nanotube actuators are papers whose pores are electrolyte filled. Strain is proportional to the square of the charge density, and the strain rate and power are proportional to current. The highly conducting nanotubes charge and discharge at the electrolyte interface. This double layer capacitance is spread throughout the actuator volume, creating a volumetric capacitance similar in magnitude to that of hexafluorophosphate-doped polypyrrole. As in conducting polymers, ions must be transported into the volume, and this rate is likely limited by electrolyte resistance and the mass transport rates within the nanotube film. The mechanisms are expected to have a similar mathematical description as those found in polypyrrole.

2.4. Fabrication and Energy Delivery

The challenges of fabrication are evident from the discussions above. Polymer films and fibers need to be thin in order to contract quickly. The spacing between electrodes should be small, and the length of polymer between electrical contacts also needs to be minimized. Such considerations suggest that conducting polymer actuators are well suited for micro and nano-scale applications. What are the challenges in creating a macroscopic motor? Creation of an artificial biceps muscle is used to emphasize some of the issues involved.

A moderate sized biceps muscle generates approximately 200 N of peak force at the hand and performs at least 45 J of work in one stroke. Given that the conducting polymers produce 5 MPa of stress and 2 % strain, a polymer volume of 4.5×10^{-4} m^3 of polymer (not including electrolyte) is required, as calculated using Equation 5. If the length is 150 mm, the cross-section must be about 55 mm × 55 mm. In order to create a full 2 % contraction in 1 s, the polymer thickness must be approximately 5 μm, as determined by the diffusion time constant, Equation 14 (half the contraction will occur within the first 0.25 s). The actuator then needs to be composed of at least 11,000 layers. If the same lever arm geometry is used as in the human forearm, then these layers must be arranged to achieve a 20 % change in actuator length. Furthermore, space must be left for the electrolyte and electrical contacts, and all the polymer surfaces must be kept within 40 mm of the counter electrode, as predicted by the volumetric $R{\cdot}C$ charging time Equation 11 (the distance must be smaller if the intervening space contains other actuator material). Equation 12 predicts that the electrical contacts to the polymer must be spaced by less than 20 mm.

The amount of charge that must be delivered to the actuator is estimated from the product of actuator volume and strain divided by the strain to charge ratio, α, following Equation 2. The average current, I_{avg}, in order to strain by ε within τ seconds is given by:

$$I_{avg} = \frac{\varepsilon \cdot Vol}{\alpha \cdot \tau}. \qquad 15$$

For the biceps muscle example the charge required is 90,000 C, to be delivered in 1 s ($\alpha = 10^{-10}$ m^3/C). This charge can be stored in two D cells, but the delivery rate is beyond the capabilities of appropriate portable power sources and wires. Over 90 % of the input energy is recoverable[8,11], but this does not preclude the delivery of high currents where fast response is needed. On the other hand, a 10^{-9} m^3 (1 mm^3) actuator only requires 200 mA to contract within 1 s. At present, moderate size to small actuator applications are the most promising for conducting polymer actuators. This will change as new materials with higher electromechanical coupling are introduced[9].

3. DISCUSSION AND CONCLUSION

Procedures are presented which enable the designer to evaluate the feasibility of incorporating hexafluorophosphate-doped conducting polymer actuators into a device, and to determine what geometries are required to enable the device to meet performance requirements.

1. Determine the maximum actuator stress that can be tolerated based on cycle time and number (Section 2.1).
2. Calculate minimum actuator volume by dividing the device work output by the polymer work density (Equation 5), where the work density is calculated by integrating the stress over strain, up to the maximum stress.
3. For a given maximum response time, calculate the polymer to counter electrode spacing, polymer thickness, and distance between contacts necessary to achieve the desired rate (Equations 8-12 and 14).
4. Estimate current and energy requirements, based on the response time and the actuator volume (Equation 15).

Many of the concepts presented are broadly applicable to other electrochemically activated conducting polymer systems. They should also help guide the user of carbon nanotube actuators, which feature many similarities with conducting polymers particularly in the underlying rate limiting mechanisms.

ACKNOWLEDGEMENTS

This work is partially supported by the Office of Naval Research. Many thanks to Patrick Anquetil and Ann Madden for their valuable comments.

APPENDIX: MODEL DERIVATION

In order to understand the ultimate performance limits of conducting polymer actuators, and to predict their response for design purposes, it is important to have models that describe actuator behavior, and provide physical insight into the underlying physical mechanisms of electro-mechanical coupling. The aim is to describe and preferably understand the process of electrical to mechanical energy transduction. A model is proposed, in which the actuator is treated as an electrolytic capacitor with the unusual feature that charging occurs throughout its volume. The rate of charging is limited by the rate of ionic diffusion into the polymer and the $R{\cdot}C$ charging. An expression for electrical admittance is derived, which, when combined with the assumption of a fixed proportionality between strain and charge, enables the prediction of stress, strain, strain rate, power to mass and efficiency as a function of input voltage or current and the applied load. Other candidate models are also put forward, and their predictions compared. Comparison of the predictions with experimental results has been performed elsewhere[8,11].

Background

Past, experimental results suggest that[8,11]:

- At long times (after several hundred seconds), voltage is proportional to the charge transferred over a range of ~ 2V;
- At short times (< 10 ms) the current is proportional to applied potential;
- Superposition and scaling of between input voltage and output current are observed;
- The magnitude of strain as a function of time/frequency suggests that diffusion is a rate-limiting factor.

These results suggest that a linear, time-invariant model is suitable to describe both the relationship between current and voltage (admittance) and between current/voltages and stress/strain. Furthermore, the impedance should look purely resistive at high frequencies, be diffusion limited at intermediate frequencies, and appear capacitive at low frequencies.

The proposed mechanisms involved in polymer charging are outlined in Figures 7 (a) through (d), which depicts a polymer electrode, an electrolyte phase and a counter electrode to each side of the polymer. Potential between the polymer and a reference electrode is set via a potentiostat. It is assumed that only anions are able to penetrate into the polymer, due to their smaller size. The application of the theory to the case of small cations and excluded anions, both ions excluded or only anions excluded is straightforward.

When a voltage is applied between the reference and the working electrode, Figure 7 (b), ions within the electrolyte are transported by electrophoretic force, with anions and cations traveling parallel to the applied field and in opposite directions.

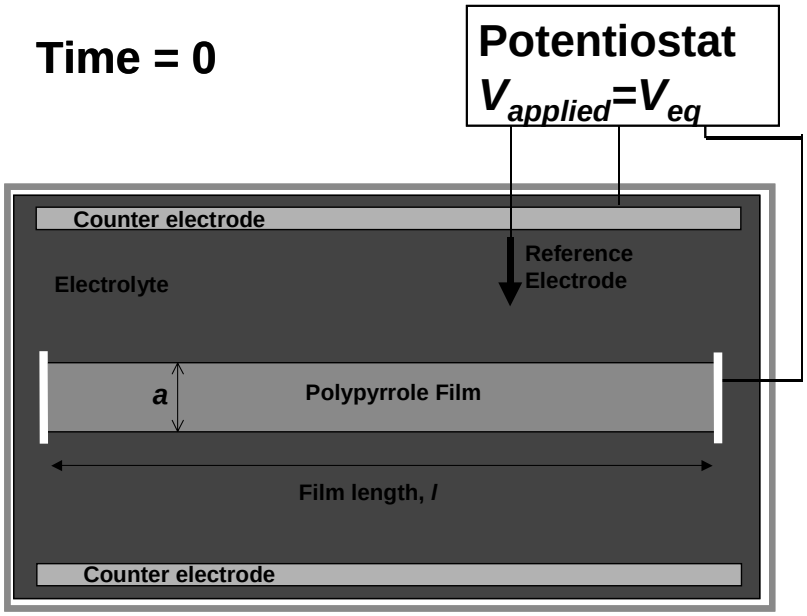

Figure 7a: Model of polypyrrole charging and Swelling (a). A polypyrrole film of thickness, *a*, immersed in an electrolyte containing small anions and bulky cations that cannot penetrate the polymer, is at equilibrium, at an applied voltage, V_{eq}.

The initial impedance is resistive in nature, and no changes in strain or stress are expected in the polymer. As depicted in Figure 7(c), these charges concentrate at the polymer/electrolyte interface. As the ions approach the interface, the polymer surface charges electronically, thereby preventing electric field from penetrating the polymer surface. The ions and charges form what is known in electrochemistry as a double layer capacitance. he spacing between ions and electronic surface charges, δ, is typically less than 30 nm in electrolytes of moderate concentration, leading to very strong fields with typical capacitances [25] of between 0.1 and 0.4 $F{\cdot}m^{-2}$. The polymer is assumed to have a much lower electronic resistance than the ionic resistance of the electrolyte and the field at its surface is assumed to be uniform, such that charging is uniform. The polymer is assumed to be porous at the molecular scale, enabling ions and solvent of sufficiently small size to enter

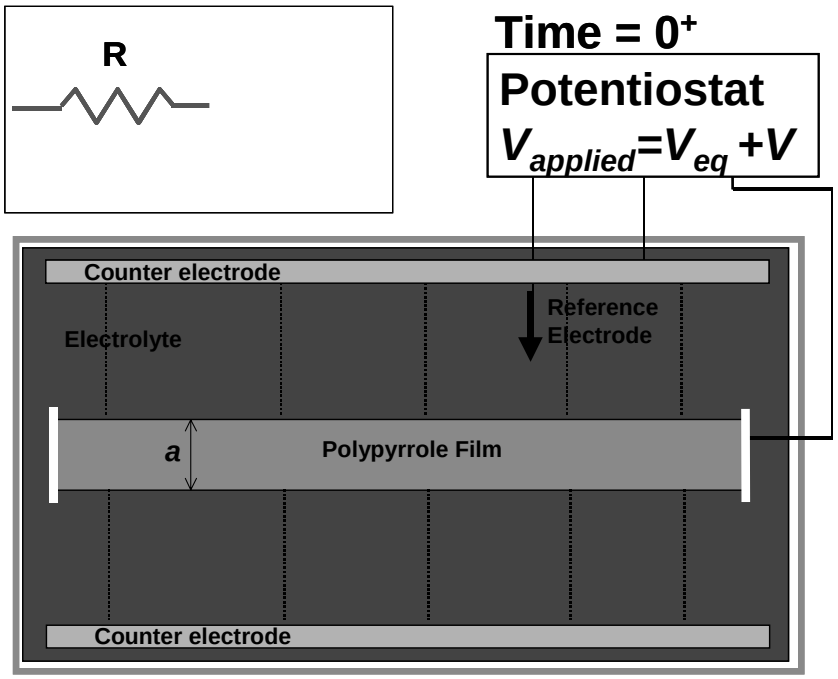

Figure 7b: Model of polypyrrole charging and Swelling (b). A potential difference, *V*, is applied, generating an electric field across the electrolyte. Ions migrate within the electrolyte and the device behaves like a resistor.

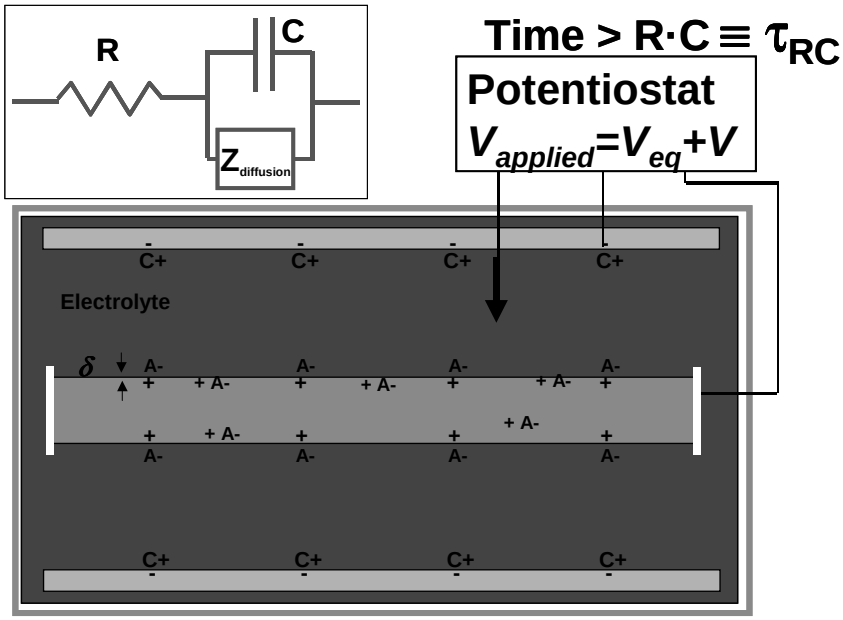

Figure 7c: Model of polypyrrole charging and Swelling (c). The migration of anions, **A-**, and cations, **C+**, leads to a build-up of ionic charge over a distance, δ, at the polymer/electrolyte interface, balanced by electronic charge, +, and forming a double layer capacitance, **C**. Some anion/charge pairs diffuse into the polymer, discharging the double layer and swelling the polymer.

and leave. The electronic conductivity of the polymer prevents fields from arising within the polymer, and thus, unlike in the electrolyte, there is no electrophoretic force on ions, and convection is not possible, so any dopant transport must occur by diffusion.

The potential difference at the polymer/electrolyte interface makes the insertion or removal of dopant/charge pairs energetically favorable. The energetics of insertion is assumed to be capacitive in nature, with the number of charges inserted proportional to the change in double layer potential. The dopant flux alters the concentration of dopant/charge pairs at the polymer surface, creating a concentration gradient within the material, which, in turn, leads to diffusion of ion/charge pairs into the polymer, Figure 7 (c). Strain rate is assumed to be directly proportional to the diffusion current. Thus, at short times/ high frequencies, strain rate is high, but drops over time, as concentration gradients are reduced. Eventually, diffusion currents permeate the entire polymer, the concentration becomes uniform and diffusion ceases, Figure 7 (d). The polymer is fully charged or discharged, and the full strain has been achieved for the given change in voltage.

Thus far the model provides qualitative explanations for all of the observations. At high frequencies and short times the behavior is resistive, owing to the solution resistance. At longer times, the double layer begins to charge and ions diffuse into the polymer. Current and strain rate are controlled by the rate of diffusion, and the extent of double layer charging. At long times, the thermodynamics determine the state, producing a capacitive response, and strain proportional to applied potential. The quantitative predictions are now investigated.

The model provides qualitative explanations for all of the observations. At high frequencies and short times the behavior is resistive, owing to the solution resistance. At longer times, the double layer begins to charge and ions diffuse into the polymer. Current and

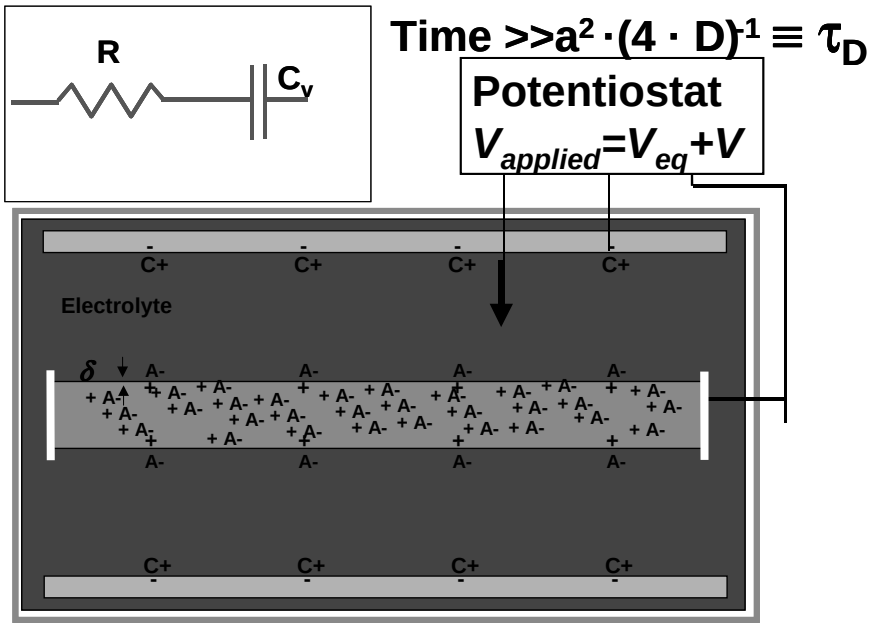

Figure 7d: Model of polypyrrole charging and Swelling (d). Diffusion slows as the concentration of ions within the polymer becomes uniform at a time $\tau_D >> a^2 \cdot (4 \cdot D)^{-1}$, where D is the anion/charge diffusion coefficient. The entire voltage drop is across the interface, but the charge is stored within the polypyrrole volume, leading to a very large effective capacitance, $\mathbf{C_V}$.

strain rate are controlled by the rate of diffusion, and the extent of double layer charging. At long times, the thermodynamics determine the state, producing a capacitive response, and strain proportional to applied potential. The quantitative predictions are now investigated.

Theory

The equations representing the diffusive-elastic-metal model are now derived. The model name stems from the assumptions that mass transport is limited by molecular diffusion within the polymer, that the polymer expands in response to ion insertions in an elastic manner, and that the polymer has a negligible electronic resistance compared to the rest of the cell, and is thus metal-like. The mechanisms of polymer electronic conduction need not be truly metallic in nature.

Assumptions

The challenge is now to represent the phenomena mathematically. The configuration to be modeled is as shown in Figure 7. A strip of polymer has a length, *l*, a width, *w*, and a thickness, *a*, in contact with an electrolyte over a surface area $A=2\times w\times l$, and is mechanically connected at each end. It is assumed that $w>>a<<l$. The mechanical connections either provide a constant force (isotonic condition) or sit a fixed distance, *l*, apart (isometric condition). Electrical contact is also made with the polymer. Voltage is applied and measured relative to an ideal voltage source also in the electrolyte (in practice provided by a combination of a reference electrode and a potentiostat). Furthermore, several assumptions are made about the nature and properties of the polymer and the electrolyte:

1. The polymer is porous, allowing ions and molecules to diffuse within it;
2. Convection and migration of ions and solvent within the polymer are negligible,;
3. Electrical contact with the polymer is characterized by a contact resistance, R_c. This resistance represents the electrical impedance arising from contact between the polymer and a metal electrode used to make electrical contact between the polymer and the potentiostat;
4. Potential drops within the polymer are negligible compared with the applied reference to polymer voltage difference;
5. The impedance of the electrolyte is characterized by a resistance, R_s. Effects of ion depletion near the polymer interface are considered to be negligible, since mass transport in the polymer is assumed to be much slower than in the electrolyte;
6. The double layer capacitance, *C*, is described by a parallel plate model, with surface area, *A*, dielectric constant, *k* and separation, δ;
7. The internal capacitance per unit volume of the polymer is equal to the double layer capacitance per unit volume, $C \cdot A^{-1} \cdot \delta^{1}$, for reasons discussed below;
8. No electron transfer (Faradaic reaction) takes place between the electrolyte and the polymer;
9. Negligible mechanical coupling exists between the polymer and the electrolyte;
10. Only a small part of the total electrical energy input creates mechanical work; and
11. All processes are linear and time invariant.

These assumptions will not hold when the polymer is in an insulating state, and thus only apply over a limited potential range. In 10, it is assumed that the electrical impedance can be modeled without regard for the coupling to mechanical energy being expended. Number 7 implies that not only are the energies per charge in the double layer and within the polymer the same, as required by thermodynamics[†], but so is the second derivative of energy with respect to charge. Why should the double layer capacitance be so closely tied to the volumetric capacitance? Double layer charging is the surface manifestation of the effect of inserting charge within the polymer, so there is no doubt that the physics of the two situations are related. There is also a large solvent content within the polymer, in the case of PPy(PF_6^-)[‡] in propylene carbonate, providing a similar dielectric environment. However, there is also a clear anisotropy at the polymer surface that is not present within the bulk. How this manifests itself will depend largely on the relative placement of charges, and solvent molecules. The symmetry of the two cases suggests that the ratio of bulk to surface capacitance will be between 1 and 2. As a first modeling attempt, the capacitances are assumed equal, thereby reducing the model complexity by one parameter, and requiring that changes in ion concentration at the double layer be matched one to one in the polymer. The assumption is tested by direct measurements of double layer capacitance. Future refinements may involve adding a factor to account for the differences in capacitances.

Several of the assumptions are not in agreement with models and results that are presented in the literature. These models and results are discussed in more detail at the end of this chapter, and differences in predicted behaviors are listed, which are then compared with experimental findings in subsequent chapters.

Derivation

In modeling the electrochemical impedance of the cell, the admittance due to diffusion and double layer charging are first derived. These elements are then related to standard lumped parameter electrochemical elements. A resistor is added to represent the solution resistance, forming a complete model. The current in response to a step change in voltage between the polymer and the reference electrode is now determined, from which the admittance transfer function (inverse of the impedance) is obtained.

The electrolyte and metal-polymer contact act as a resistance, $R=R_c+R_s$, and the interface between the polymer and the electrolyte as a double layer capacitance, C. Current, I, passing though the cell must traverse the electrolyte. The current charges the double layer capacitance, which is simultaneously discharged by diffusion of ion/electronic carrier pairs into the polymer. Diffusion is driven by concentration gradients, whereas ionic currents and double layer charging are driven by potential gradients. These 'forces' are now related, and an expression for the admittance, Y, is obtained in terms of :

- Circuit resistance, $R=R_s+R_c$,
- Double layer capacitance, C,
- Polymer thickness, a,
- Polymer surface area, $A=2\times w\times l$,
- Coefficient of ionic diffusion in the polymer, D,
- Double layer separation, δ,
- and the Laplace variable, s.

Intermediate variables and constants include:

- the double layer charging current, I_c,
- the diffusion current, I_D,
- the ionic concentration within the polymer as a function of position and time, $c(x,t)$,
- and the Faraday constant, $F = 9.64846\cdot10^4$ Coulombs per mole.

Figure 5 is a schematic of the model circuit, including Z_D, the diffusion impedance for a film of finite thickness.
The total cell current, $I(t)$, is the sum of the diffusion and double layer charging currents:

$$I(t) = I_C(t) + I_D(t), \qquad 16$$

and the total potential drop is:

[†] Interactions between particles both within the polymer and the double layer are assumed to determine the population of states, with entropy playing a minimal role. The presence of very strong electrostatic forces and the capacitive behavior observed over potential ranges of more than 1 V are used to justify this assertion in further discussions below.

[‡] Represents polypyrrole doped with hexafluorophosphate anions used in this study.

$$V(t) = I(t) \cdot R + \frac{1}{C} \cdot \int_0^t I_C(t) dt \,. \qquad 17$$

The diffusion current, I_D, at the polymer/electrolyte interface is given by Fick's first law:

$$I_D(t) = -F \cdot A \cdot D \cdot \left. \frac{\partial c}{\partial x}(x,t) \right|_{x=0}, \qquad 18$$

where x is position within the polymer, with x=0 at the polymer/electrolyte interface, and x increasing normal to the interface and into the polymer. The double layer charging current is:

$$I_C(t) = F \cdot A \cdot \delta \cdot \left. \frac{\partial c}{\partial t}(x,t) \right|_{x=0}. \qquad 19$$

In this last equation the double layer is described as having a thickness, δ, and an area, A, in which the average ionic concentration is varying in time.

One more equation is required, which must relate concentration gradient at the interface to the time rate of change in concentration. The relationship between the two is obtained by convolving the response to a step change in concentration at the boundary with the rate of change in surface concentration. The concentration profile as a function of time, in a film of thickness, a, in response to a step change in concentration, c_o, at x=0 and x=a, is:

$$\frac{c(x,t)}{c_o} = \left[1 - \frac{4}{\pi} \cdot \sum_{n=0}^{\infty} \frac{\sin(\pi \cdot (2 \cdot n + 1) \cdot x \cdot a^{-1}) \cdot \exp(-\pi^2 \cdot (2 \cdot n + 1)^2 \cdot D \cdot t \cdot a^{-2})}{2 \cdot n + 1} \right] = B(x,t) \,. \qquad 20$$

To obtain this result, the initial concentration profile (constant concentration across the film, zero at the edges) is expanded as a Fourier series. Separation of variables is employed to solve the one-dimensional diffusion equation given the boundary and initial conditions.

Next, the superposition principle is applied in the form of the convolution integral such that the concentration profile can be obtained for a nearly arbitrary choice of boundary concentrations with time:

$$c(x,t) = \int_0^t \frac{\partial c(0, t-\tau)}{\partial \tau} \cdot B(x,\tau) d\tau \,. \qquad 21$$

The use of the step response rather than the impulse response in the convolution integral eliminates the appearance of singularities later in the derivation.

According to Fick's First Law, the diffusion current is proportional to the gradient in concentration, which, at x=0 (or equivalently x=a) is:

$$\frac{\partial c}{\partial x}(0,t) = -\frac{4}{a} \cdot \int_0^t \frac{\partial c(0, t-\tau)}{\partial \tau} \cdot \sum_{n=0}^{\infty} \exp\left(\frac{-\pi^2 \cdot (2 \cdot n + 1)^2 \cdot D \cdot \tau}{a^2}\right) \cdot d\tau \,. \qquad 22$$

This system of equations (1,2,3,4,7) is transformed into the Laplace domain:

$$I(s) = I_C(s) + I_D(s) \,, \qquad 23$$

$$V(s) = I(s) \cdot R + \frac{1}{s \cdot C} \cdot I_C(s), \qquad 24$$

$$I_D(s) = -F \cdot A \cdot D \cdot \left. \frac{\partial c}{\partial x}(x,s) \right|_{x=0}, \qquad 25$$

$$I_C(s) = F \cdot A \cdot \delta \cdot s \cdot c(0,s) \,, \text{ and} \qquad 26$$

$$\frac{\partial c}{\partial x}(0,s) = -\frac{4}{a}\cdot c(0,s)\cdot s\cdot\sum_{n=0}^{\infty}\frac{1}{s+\frac{\pi^2\cdot(2n+1)^2\cdot D}{a^2}}. \qquad 27$$

Solving for the admittance, $Y(s)$, as a function of the Laplace variable, s, the material thickness, a, the diffusion coefficient, D, the electrolyte and contact resistance, R, the double layer capacitance, C and the double layer thickness, δ, yields:

$$Y(s)\cdot R = \frac{1}{1+\frac{1}{R\cdot C\cdot s\left[1+\frac{4\cdot D}{a\cdot\delta}\cdot\sum_{n=0}^{\infty}\frac{1}{s+\pi^2(2\cdot n+1)^2\cdot D\cdot a^{-2}}\right]}} = \frac{I(s)\cdot R}{V(s)}. \qquad 28$$

Making use of the expansion:

$$\frac{\tanh\left(\frac{1}{2}\cdot\sqrt{\frac{s}{x}}\right)}{4\cdot\sqrt{x\cdot s}} = \sum_{n=0}^{\infty}\frac{1}{s+\pi^2\cdot(2\cdot n+1)^2\cdot x}, \qquad 29$$

leads to the relationship:

$$Y(s)\cdot R = s\cdot\frac{\frac{\sqrt{D}}{\delta}\cdot\tanh(\frac{a}{2}\cdot\sqrt{\frac{s}{D}})+\sqrt{s}}{\frac{\sqrt{s}}{R\cdot C}+s^{3/2}+\frac{\sqrt{D}}{\delta}\cdot s\cdot\tanh(\frac{a}{2}\cdot\sqrt{\frac{s}{D}})}. \qquad 30$$

In this form there are four parameters to be determined, namely the capacitance, C, the diffusion coefficient, D, the double layer thickness, δ, and the resistance, R. The double layer capacitance, C, can be approximately related to δ by assuming a parallel plate capacitor, of area, A, dielectric constant, k, permittivity of free space, ε_o, and plate spacing, δ:

$$\delta = \frac{k\cdot\varepsilon_o\cdot A}{C}. \qquad 31$$

A parallel plate model of double layer capacitance (Helmholtz plane) generally provides a good approximation [25] at electrolyte concentrations of 0.05 M and above in high dielectric constant solvents. The dielectric constant is taken to be that of the electrolyte. Film dimensions are readily measured. The unknowns are now reduced to three: the resistance, R, the double layer capacitance, C and the diffusion coefficient, D.

Next the equivalence to standard elements used in electrochemical impedance models is demonstrated. Setting R=0 leaves the diffusion and double layer capacitance terms of the admittance:

$$Y(s) = \frac{\sqrt{D}\cdot C}{\delta}\cdot\sqrt{s}\cdot tanh(\frac{a}{2}\cdot\sqrt{\frac{s}{D}})+C\cdot s. \qquad 32$$

The second term on the right is the admittance of the double layer capacitance. The first term has the same form as the admittance of a finite $R\cdot C$ transmission line, which is represented as[27]:

$$Y_o\cdot\sqrt{s}\cdot tanh(B\cdot\sqrt{s}), \qquad 33$$

where:

$$B = \sqrt{\frac{a^2}{4\cdot D}}, \text{ and } Y_o = \sqrt{\frac{D}{\delta^2}}\cdot C = \frac{\sqrt{D}}{k\cdot\varepsilon\cdot A}\cdot C^2. \qquad 34$$

REFERENCE LIST

1. T. A. Skotheim, R. L. Elsenbaumer, J. R. Reynolds, *Handbook of Conducting Polymers*, 2nd ed., Marcel Dekker, New York, 1998.
2. E. T. Jones, E. Chao, M. J. Wrighton, "Preparation and Characterization of Molecule-Based Transistors With a 50 Nm Separation", *Journal of the American Chemical Society* **109**, pp. 5526-5529, 1987.
3. R. H. Baughman, R. L. Shacklette, R. L. Elsenbaumer, "Micro Electromechanical Actuators based on Conducting Polymers", *Topics in Molecular Organization and Engineering: Molecular Electronics*, P. I. Lazarev, Ed., vol. 7, pp.267, Kluwer, Dordrecht, 1991.
4. Q. Pei and O. Inganas, "Electrochemical Applications of the Beam Bending Method; a Novel Way to Study Ion Transport in Electroactive Polymers", *Solid State Ionics* **60**, pp. 161-166, 1993.
5. A. Mazzoldi, A. Della Santa, D. De Rossi, "Conducting polymer actuators: Properties and modeling", *Polymer Sensors and Actuators*, Y. Osada and D. E. De Rossi, Eds., Springer Verlag, Heidelberg, 1999.
6. A. S. Hutchison, T. W. Lewis, S. E. Moulton, G. M. Spinks, G. G. Wallace, "Development of Polypyrrole-Based Electromechanical Actuators", *Synthetic Metals* **113**, pp. 121-127, 2000.
7. T. F. Otero, "Artificial Muscles, electrodissolutoin and redox processes in conducting polymers", *Handbook of organic and conductive molecules and polymers*, H. S. Nalwa, Ed., vol. 4, pp.517-594, John Wiley & Sons, Chichester, 1997.
8. J. D. Madden, P. G. Madden, I. W. Hunter, "Characterization of polypyrrole actuators: modeling and performance", *Proceedings of SPIE 8th Annual Symposium on Smart Structures and Materials: Electroactive Polymer Actuators and Devices*, Yoseph Bar-Cohen, Ed., pp.72-83, SPIE, Bellingham WA, 2001.
9. P. A. Anquetil et al., "Thiophene based conducting polymer artificial muscles", *Proceedings of SPIE 9th Annual Symposium on Smart Structures and Materials: Electroactive Polymer Actuators and Devices*, Yoseph Bar-Cohen, Ed., SPIE, Bellingham WA, 2002.
10. J. D. Madden, R. A. Cush, T. S. Kanigan, I. W. Hunter, "Fast Contracting Polypyrrole Actuators", *Synthetic Metals* **113**, pp. 185-193, 2000.
11. J. D. Madden, "Conducting Polymer Actuators", *Ph.D. Thesis*, Massachusetts Institute of Technology, Cambridge, MA, 2000.
12. G. M. Spinks, G. G. Wallace, L. Liu, D. Zhou, "Conducting polymers and carbon nanotubes as electromechanical actuators and strain sensors", *Materials Research Symposium Proceedings*, Bar-Cohen, Ed., vol. 698, pp.EE1.1.1 -EE1.1.12, Materials Research Society, 2002.
13. J. D. Madden, R. A. Cush, T. S. Kanigan, C. J. Brenan, I. W. Hunter, "Encapsulated Polypyrrole Actuators", *Synthetic Metals* **105**, pp. 61-64, 1999.
14. R. H. Baughman, "Conducting Polymer Artificial Muscles", *Synthetic Metals* **78**, pp. 339-353, 1996.
15. J. D. Madden, P. G. Madden, P. A. Anquetil, I. W. Hunter, "Load and Time Dependence of Displacement in a Conducting Polymer Actuator", *Materials Research Symposium Proceedings*, Bar Cohen, Ed., vol. 698, pp.EE4.3.1 - EE4.3.8, Materials Research Society, 2002.
16. R. M. Penner and C. R. Martin, "Electrochemical Investigations of Electronically Conductive Polymers. 2. Evaluation of Charge-Transport Rates in Polypyrrole Using an Alternating Current Impedance Method.", *Journal of Physical Chemistry* **93**, pp. 984-989, 1989.
17. R. A. Bull, F.-R. F. Fan, A. J. Bard, "Polymer Films on Electrodes", *Journal of the Electrochemical Society* **129**, pp. 1009-1015, 1982.
18. Ren, Xiaoming and Pickup, Peter G. The origin of the discrepancy between the low frequency AC capacitances and voltammetric capacitances of conducting polymers. Journal of electroanalytical chemistry 372, 289-291. 94.
19. J. J. Kim, T. Amemiya, D. A. Tryk, K. Hashimoto, A. Fujishima, "Charge Transport Processes in Electrochemically Deposited Poly(Pyrrole) and Poly(N-Methylpyrrole) Thin Films", *Journal of Electroanalytical Chemistry* **416**, pp. 113-119 , 1996.
20. T. Yeu, T. V. Nguyen, R. E. White, "A Mathematical Model for Predicting Cyclic Voltammograms of Electrically Conductive Polypyrrole", *Journal of the Electrochemical Society: Electrochemical Science and Technology* pp. 1971-1976, 1988.
21. H. Mao, J. Ochmanska, C. D. Paulse, P. G. Pickup, "Ion Transport in Pyrrole-Based Polymer Films", *Faraday Discussions of the Chemical Society* **88**, pp. 165-176, 1989.
22. J. Tanguy, N. Mermilliod, M. Hocklet, "Capacitive Charge and Noncapacitive Charge in Conducting Polymer Electrodes", *Journal of the Electrochemical Society: Electrochemical Science and Technology* pp. 795-801, 1987.
23. Posey, F. A. and Morozumi, T. Theory of potentiostatic and galvanostatic charging of the double layer in poirous electrodes. Journal of the Electrochemical Society 113(2), 176-184. 66.
24. A. Della Santa, A. Mazzoldi, C. Tonci, D. De Rossi, "Passive Mechanical Properties of Polypyrrole Films: a Continuum Poroelastic Model", *Materials Science and Engineering C* **5**, pp. 101-109, 1997.
25. A. J. Bard and L. R. Faulkner, *Electrochemical Methods, Fundamentals and Applications*, Wiley, New York, 1980.
26. J. C. Lacroix, K. K. Kanazawa, A. Diaz, "Polyaniline: A Very Fast Electrochromic Material", *Journal of the electrochemical society* **136** , pp. 1308-1313, 1989.
27. B. A. Boukamp, "A Nonlinear Least Squares Fit Procedure for Analysis of Immittance Data of Electrochemical Systems", *Solid State Ionics* **20**, pp. 31-44, 1986.